Thermal bit writing simulations in magneto-optic recording media

doi: 10.1109/20.800688

Thermal bit writing simulations in magneto-optic recording media

S.J. Greaves, H. Muraoka, Y. Sugita and Y. Nakamura
RIEC, Tohoku University, Katahira 2-1-1, Aoba ku, Sendai, 980-8577, Japan.

***Abstract*—A micromagnetic simulation based on the Landau-Lifshitz-Gilbert equation includes random field terms to represent thermal effects. By recalculating the temperature of each cell in the simulation at each time step the effects of localised heating by a laser and of heat conduction can be included in the calculations. This allows a simulation of magneto-optic recording processes to be carried out. Single bit nucleation in zero field was simulated, as were written tracks.**

***Index Terms*—Magneto-optic, nucleation, simulation.**

I. Introduction

Magnetic media were simulated using the solution of the Landau-Lifshitz-Gilbert (LLG) equation.

$$\frac{d\vec{M}}{dt} = -\gamma\left(\vec{M} \wedge \left(\vec{H} - \frac{\alpha}{\gamma M_s}\cdot\frac{d\vec{M}}{dt}\right)\right). \quad (1)$$

The solution of (1) gives the relationship between the magnetisation and time. Here, $\vec{M}$ is the magnetisation, $\vec{H}$ the effective field acting on the magnetic moment, α a damping constant and γ the gyromagnetic ratio. By including a random field component in the calculation of the effective field thermal effects can be simulated [1]. The effective field is then given by

$$\vec{H} = \vec{H}_d + \vec{H}_{ex} + \vec{H}_{ku} + \vec{H}_{app} + \vec{H}_{th} \quad (2)$$

where the components of $\vec{H}$ in (2) represent the demagnetising field, exchange field, uniaxial anisotropy field, external applied field and the random field respectively. The random field components take a Gaussian distribution whose time-average is zero. The random field is related to the temperature, θ, by the equation [2]

$$\sigma = \sqrt{\frac{2k_b\theta\alpha}{VM_s\gamma dt}} \quad (3)$$

with σ being the standard deviation of the distribution of random fields, k_b the Boltzmann constant, V the volume of material, M_s the saturation magnetisation and dt the time step. In a typical simulation the magnetic medium is divided into small cells, in this way it is possible to simulate localised heating of the medium, e.g. heating due to a laser pulse etc, by assigning a unique temperature to each cell and recalculating the temperature at each time step of the simulation.

In a simulation of magneto-optic recording there are two influences on the medium temperature to be considered: heating due to the laser pulse and heat conduction from neighbouring cells, including the substrate or air surface where appropriate. For a normally incident laser beam of intensity I(0) the intensity at a depth, z, in the magnetic film is given by

$$I(z) = (1-R)I(0)\exp\left(\frac{-4\pi K_0}{\lambda}z\right) \quad (4)$$

where R is the reflectance of the medium, λ the laser wavelength and K_0 the extinction coefficient of the medium. Eq. (4) can easily be integrated to give the average intensity through the depth of the i'th cell thus:

$$I_{ave}(i) = \frac{(1-R)I(0)}{\delta z_i}\int_{z_i\,\max}^{z_i\,\min}\exp\left(\frac{-4\pi K_0}{\lambda}z\right)dz \quad (5)$$

here δz_i is the thickness of cell i, and $z_i$min and $z_i$max are the distances from the film surface to the top and bottom of cell i respectively. If the cell has a specific heat capacity per unit volume of C and $I_{ave}(i)$ is expressed in Watts then the temperature increase, $d\theta$, during each time step due to the laser heating is given by

$$d\theta_i(laser) = \frac{I_{ave}(i)dt}{C_iV_i}. \quad (6)$$

Next we consider the heat flow from neighbouring cells. We use the heat flow equation

$$Q_{ij} = \mathrm{K}A_{ij}\frac{\theta_j - \theta_i}{L_{ij}}dt \quad (7)$$

to calculate the flow of heat into cell i from cell j per time step. In (7) K is the heat conduction constant, A_{ij} the common surface area of the two cells, θ_i and θ_j the temperature of the cells and L_{ij} the centre-centre distance between the cells. For each cell, the heat flow to and from adjacent cells is calculated at each time step of the simulation and the temperature adjusted accordingly. The temperature change in cell i due to its neighbours, j, is given by

$$d\theta_i(flow) = \frac{\mathrm{K}dt}{C_iV_i}\sum_j\frac{A_{ij}(\theta_j - \theta_i)}{L_{ij}}. \quad (8)$$

Manuscript received : February 26, 1999.
S.J. Greaves, simon@kiroku.riec.tohoku.ac.jp

Thus we can calculate the temperature change of each cell at each step in the simulation as the sum of (6) and (8).

For the calculations the following parameters were used. The medium specific heat and conduction constants are those for cobalt [3]. The M_s and K_u values were intended to represent a Co-based thin film multilayer. One surface of the medium was assumed to be air and the other surface a glass substrate. The ambient temperature outside of the computing region was set at 300K. The time step in the simulations was 5.68×10^{-13}s and the damping constant was 0.05. In addition, the uniaxial anisotropy was assumed to decrease linearly from 1×10^{6} erg/cc at 300K to zero at the Curie temperature. The laser beam had a Gaussian intensity profile, the radius of the beam is defined here as the distance from the beam centre to where the beam intensity is one half of the maximum intensity.

TABLE I CALCULATION PARAMETERS

Medium thickness (Å)	100
Saturation magnetisation, M_s, (emu/cm^3)	300
Uniaxial anisotropy, K_u (300K), (erg/cm^3)	1×10^{6}
Exchange constant, A, (erg/cm)	$0\text{-}1\times10^{-6}$
Specific Heat, C, (J/cm^{3}K)	3.67
Conduction constant, K, (W/cmK)	1
Conduction constant (air) (W/cmK)	1.37×10^{-5}
Conduction constant (substrate) (W/cmK)	0.01
Reflectance	0.7
Extinction coefficient, K_0	4
Laser wavelength, λ, (Å)	6330
Ambient temperature (K)	300
Curie temperature (K)	500

II. Results

The incident laser power, P, was set at 23mW, focused to a spot of radius r_l=0.15μm. The laser pulse length, t_{on}, was equal to 1000 calculation cycles (0.57ns). The simulation was run for a further 2.28ns (t_{off}) after the end of the laser pulse. We began with a saturated medium and attempted to simulate nucleation of bits in zero applied field. Fig. 1 shows the nucleated bits at the end of the simulation for various exchange coupling strengths.

Bits were nucleated for all values of exchange coupling. For exchange coupling constants greater than 5×10^{-7} erg/cm the nucleated bit disappeared as the medium cooled. For the media with exchange coupling constants up to 1×10^{-7} erg/cm the nucleated bits were non-continuous regions in which the moments of cells reversed individually. As the exchange coupling increased, the continuously nucleated regions grew larger eventually forming a single, continuous region.

Fig. 2 shows the radius of the nucleated bits, calculated from the decrease in magnetisation of the medium, at the end of the simulation and also at the point where the decrease in magnetisation from saturation was a maximum. We find that the maximum bit size occurs for A between 2.5×10^{-7} erg/cm and 5×10^{-7} erg/cm, although only towards the higher values of A do the bits consist of a continuous, uniformly magnetised region.

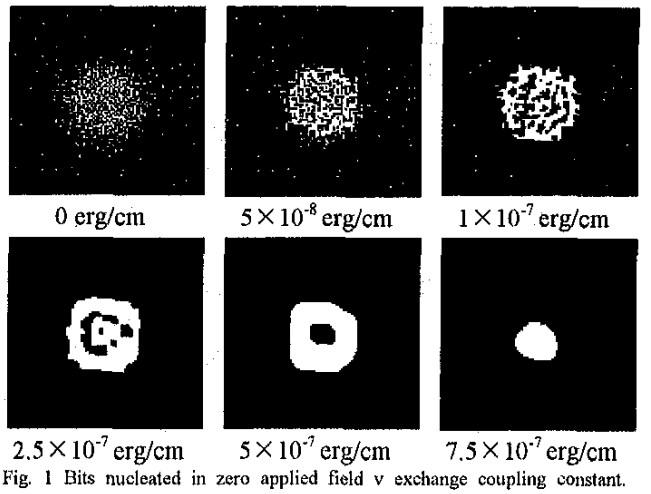

Fig. 1 Bits nucleated in zero applied field v exchange coupling constant. P=23mW, t_{on}=0.57ns, laser spot radius=0.15μm. Depicted area=1μm × 1μm.

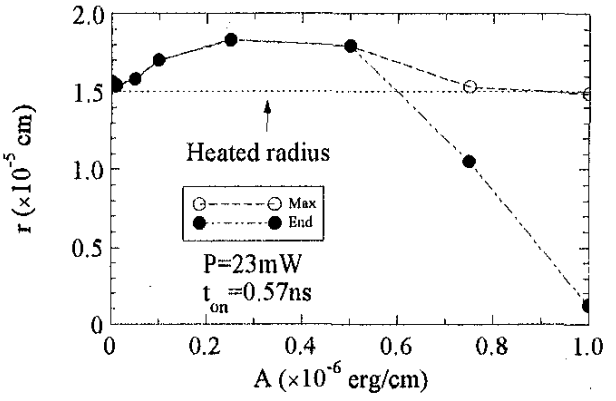

Fig. 2 Maximum radius of nucleated bits and radius at end of simulation v exchange constant. Parameters as for fig. 1.

Next, the exchange constant was set at 5×10^{-7} erg/cm and the pulse length was varied. Fig. 3 shows the radius of the nucleated bits against the pulse duration. We find that the bit size does not increase significantly for longer pulse lengths. This is probably due to the fact that the magnetostatic fields which drive the creation of the nucleated bit are decreasing in strength as the bit size increases. For pulse durations less than 0.2ns the temperature of the medium is not increased sufficiently for a bit to nucleate. Also shown in fig. 3 is the nucleated bit radius versus the incident laser power. We find that there is a threshold power of about 10mW above which the bit size increases with laser power.

Fig. 4 depicts nucleated bit radii for various laser spot radii, the laser power was constant in each case. For a given set of conditions there will be an upper limit to the spot radius beyond which a bit will not be nucleated. In this example, for a spot radius greater than about 0.25μm the laser power is too diffuse to heat the medium sufficiently and induce bit nucleation. The fig. also shows the nucleated bit radii

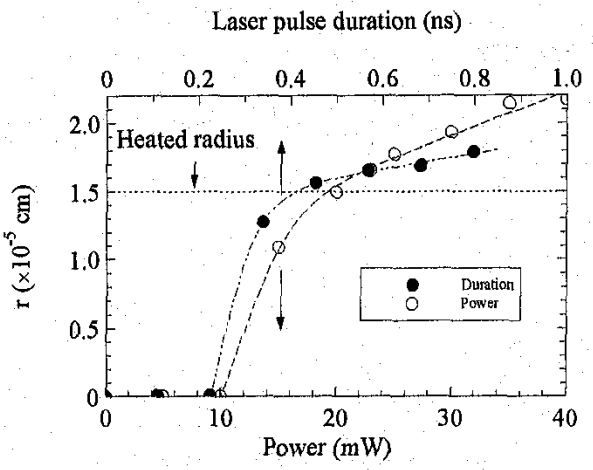

Fig. 3 Radius of nucleated bits at the end of the simulation versus laser pulse duration (P=23mW) and laser power (t_{on}=0.57ns). Laser spot radius=0.15μm, A=5×10^{-7} erg/cm. H_{app}=0.

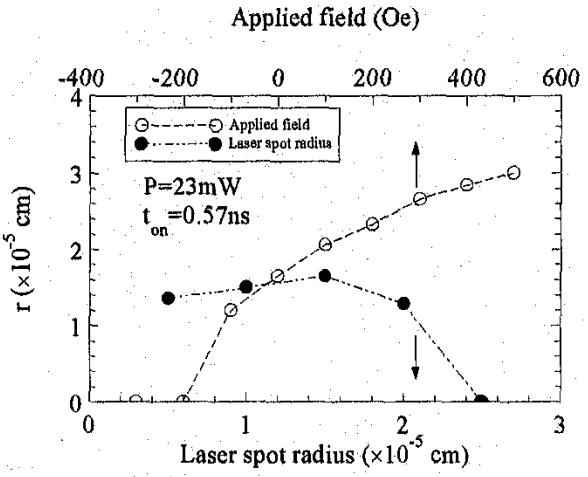

Fig. 4 Radius of nucleated bits at the end of the simulation for different laser spot radii (H_{app}=0) and applied field during writing (r_l=0.15μm). Laser power=23mW, pulse length=0.57ns, A=5×10^{-7} erg/cm.

obtained when writing was accompanied by an external applied field. The field was applied over the whole of the simulation region for the whole of the calculation time. We find a strong dependence of the bit radius on the applied field strength. A field of -200 Oe is required to prevent the nucleation of a bit. In this field a bit is initially nucleated but is subsequently erased once the laser pulse ends.

We attempted to write tracks of multiple bits in a medium using external applied fields to alternate the direction of magnetisation of the bits in the track. Since the medium with A=5×10^{-7} erg/cm has a high susceptibility to magnetic fields we reduced A to 2.5×10^{-7} erg/cm for the multiple bit-writing simulations. We moved the laser spot along the length of the track at a constant speed and used writing conditions of P=23mW, r_l=0.15μm, t_{on}=0.57ns, t_{off}=1.71ns. This corresponds to about 440 Mbit/s at a linear density of 127 kfci and a head-medium velocity of around 88 m/s. Fig. 5 shows a track written in fields of ±500 Oe. The bits are

Fig.5 Written bits at 127 kfci. P=23mW, r_l=0.15μm, H_{app}=±500Oe, A=2.5×10^{-7} erg/cm. Depicted area=1μm×2μm.

clearly defined and have the crescent shape typical of thermally recorded bits. The track width is about 0.5μm.

We calculated the likely outputs from the recorded tracks by assuming a Kerr rotation proportional to M_z, the perpendicular component of magnetisation, and a focused readout laser beam with a radius of 0.15μm and a Gaussian intensity distribution. We ran the beam along the length of the track and calculated the signal which would be seen by the detector. Fig. 6 shows the results. There is a broad range of fields, from 300 Oe to 500 Oe, over which the output is at a plateau.

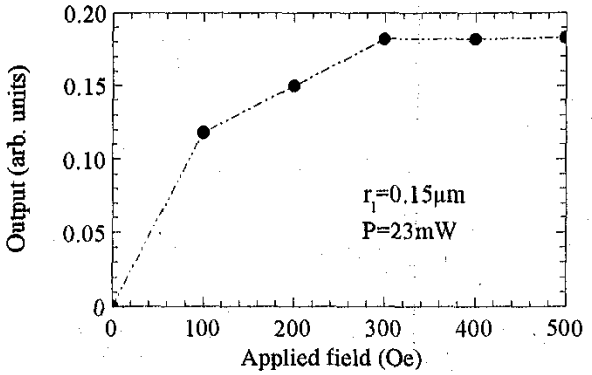

Fig. 6 Calculated outputs v applied field obtained from multiple bit written tracks. Readout laser spot radius=0.15μm.

III. Conclusions

We discussed how magneto-optic recording can be simulated using standard micromagnetic techniques and showed examples of bit nucleation in zero field and of multiple bit recording. We expect that this method can easily be extended to allow for the simulation of more complex structures e.g. those incorporating reflective layers etc.

References

[1] W.F. Brown, "Thermal fluctuations of fine ferromagnetic particles", *IEEE Trans. Magn.*, vol. 15, pp. 1196-1208, 1979.
[2] H.N. Bertram and Q. Peng, "Numerical simulations of the effect of record field pulse length on medium coercivity at finite temperatures", *IEEE Trans. Magn.*, vol. 34, pp. 1543-1545, 1998.
[3] CRC Handbook of Chemistry and Physics, CRC Press, 1972.